

Geometric phase for twisted photons

Li-Ping Yang^{1,*}

¹Center for Quantum Sciences and School of Physics, Northeast Normal University, Changchun 130024, China

We use a purely geometric method to understand the rotation of the photonic polarization vector in an optical fiber without birefringence. This rotation was explained due to Berry's phase of spin-1 photons. Via our method, we predict similar geometric rotations also exist for twisted photons carrying orbital angular momentum (OAM). The corresponding geometric phase can be applied in photonic OAM-state-based quantum computation and quantum sensing.

In the 1980s, the geometric rotation of the polarization vector of light was observed in a helically wound single-mode fiber by Ross [1] and other researchers [2]. This phenomenon was later explained due to the Berry's phase [3] $\gamma(C) = -2\pi m_s(1 - \cos \theta)$ of spin-1 ($m_s = 1$) photons traveling on a helix with pitch angle θ by Chiao and Wu [4]. Tomita and Chiao experimentally verified this photonic Berry's phase of more general fiber configurations with non-uniform torsion [5]. In Chiao and Wu's quantum description [4], the helicity of photons $\hat{S} \cdot \mathbf{k}/|\mathbf{k}|$, which is the projection of photon spin on the wave vector \mathbf{k} axis, is an adiabatic invariant during propagation. Thus, the photon spin states could accumulate Berry's phase when moving in the parameter (reciprocal) space. Berry constructed a Schrödinger-like equation with an effective photon-spin Hamiltonian for electromagnetic fields propagating in a mono-mode fiber to complete this quantum interpretation [6]. In addition to the photon helicity, the projection of the photonic OAM $\langle \hat{L} \cdot \mathbf{e}_z \rangle$ on the propagating direction \mathbf{e}_z is also conserved [7, 8]. An interesting question arises does a similar geometric rotation exist for the OAM degrees of freedom of photons? In this work, we show the answer is yes.

In parallel to the quantum Berry-phase-based description [4, 6], classical geometric interpretations of the anholonomy of coiled light have also been proposed [1, 9, 10]. Inspired by these insights, we give a different explanation for this rotation by combining differential geometry of the coiled fiber path and reflections of photons in the fiber. The key idea is to evaluate the rotation of the photon coordinate frame (PCF) with respect to the local coordinate frame (LCF) parallelly transporting on the fiber. We prove that the LCF always recovers its initial configuration after one circulation if the two ends of the fiber are parallel. Then, the rotation of the PCF leads to the rotation of the polarization of the light, i.e., the previous geometric phase of photon spin states [4]. Applying our theory on a twisted photon, we predict that a photon carrying OAM $m\hbar$ will acquire a geometric phase $\gamma_m(C) = 2m\pi \cos \theta$ after one helical circulation.

Parallel transport of the local coordinate frame—The unit tangent vector $\mathbf{t}(s)$, normal vector $\mathbf{n}(s)$, and binormal vector $\mathbf{b}(s)$ form a LCF on the fiber at s as shown in Fig. 1 (a). When a curve is parametrized by the arc length s , the dynamics of

the LCF is governed by Frenet formulas [11]

$$\frac{d}{ds} \mathbf{n}(s) = -\kappa(s)\mathbf{t}(s) - \tau(s)\mathbf{b}(s), \quad (1)$$

$$\frac{d}{ds} \mathbf{b}(s) = \tau(s)\mathbf{n}(s), \quad (2)$$

$$\frac{d}{ds} \mathbf{t}(s) = \kappa(s)\mathbf{n}(s), \quad (3)$$

where $\kappa(s)$ and $\tau(s)$ are the curvature and torsion of the curve at s , respectively.

For a uniform helix, its curvature κ and torsion τ are constants. A helix is usually described by the parametric vector [11],

$$\mathbf{r}(s) = \left(a \cos \frac{s}{c}, a \sin \frac{s}{c}, b \frac{s}{c} \right), \quad (4)$$

where $c^2 = a^2 + b^2$ and the parameters are connected to the curvature and torsion via

$$\kappa = \frac{a}{c^2}, \quad \tau = \frac{b}{c^2}. \quad (5)$$

We can re-parameterize the helical curve with the azimuthal angle $\varphi = s/c = \omega s$ with $\omega = \sqrt{\kappa^2 + \tau^2} = 1/c$. We note that ω is the angular frequency with respect to the the azimuthal angle φ and it is not the frequency of photons. The uniform helix is now described by

$$\mathbf{r}(\varphi) = \frac{1}{\omega^2} (\kappa \cos \varphi, \kappa \sin \varphi, \tau \varphi). \quad (6)$$

One round trip of photons in Ref. [4] corresponds to our azimuthal angle φ varying from 0 to 2π .

The dynamic evolution of the LCF on a uniform helix is given by,

$$\hat{R}(\varphi, \mathbf{e}) = \begin{bmatrix} \cos \varphi & -\cos \theta \sin \varphi & -\sin \theta \sin \varphi \\ \cos \theta \sin \varphi & \sin^2 \theta + \cos^2 \theta \cos \varphi & -\sin \theta \cos \theta (1 - \cos \varphi) \\ \sin \theta \sin \varphi & -\sin \theta \cos \theta (1 - \cos \varphi) & \sin^2 \theta \cos \varphi + \cos^2 \theta \end{bmatrix}, \quad (7)$$

which is the rotation around the axis $\mathbf{e} = [0, -\sin \theta, \cos \theta]$ with $\sin \theta = \kappa/\omega$ and $\cos \theta = \tau/\omega$. We can verify that $\hat{R}(2\pi, \mathbf{e})$ equals to the identity matrix \hat{I} . Thus, the LCF returns its initial configuration in the stationary laboratory reference frame. Next, we will show that this result is still valid for a non-uniform helix if two ends of the curve are parallel.

* lipinyang87@gmail.com

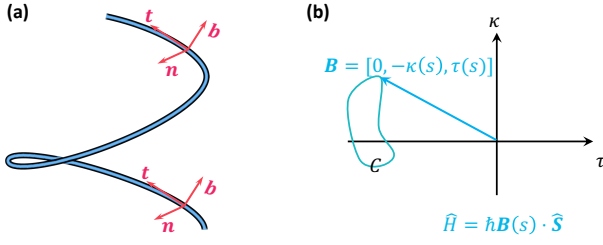


FIG. 1. (a) Parallel transport of the local coordinate frame (LCF) on a curve. (b) Movement of the LCF in the parameter space described by the effective magnetic field $\mathbf{B}(s) = [0, -\kappa(s), \tau(s)]$ and Hamiltonian $\hat{H} = \hbar \mathbf{B} \cdot \hat{\mathbf{S}}$. Here, $\kappa(s)$ and $\tau(s)$ are the local curvature and torsion of the curve at s , and $\hat{\mathbf{S}}$ is an operator vector composed of generators of the SO(3) rotations as given in Eq. (10).

Considering an arbitrary vector $\mathbf{v} = v_n \mathbf{n} + v_b \mathbf{b} + v_t \mathbf{t}$ co-moving with the LCF, we can express its motion equation in a Schrödinger-like form

$$i\hbar \frac{d}{ds} |\psi_{\mathbf{v}}(s)\rangle = \hat{H}(s) |\psi_{\mathbf{v}}(s)\rangle, \quad (8)$$

where $|\psi_{\mathbf{v}}(s)\rangle = [v_n(s), v_b(s), v_t(s)]^T$ and the effective Hamiltonian is given by

$$\hat{H}(s) = \hbar \mathbf{B}(s) \cdot \hat{\mathbf{S}}, \quad (9)$$

with an effective magnetic field $\mathbf{B}(s) = -\kappa(s)\mathbf{b}(s) + \tau(s)\mathbf{t}(s)$ and the generators of the SO(3) rotations

$$\hat{S}_n = \begin{bmatrix} 0 & 0 & 0 \\ 0 & 0 & -i \\ 0 & i & 0 \end{bmatrix}, \quad \hat{S}_b = \begin{bmatrix} 0 & 0 & i \\ 0 & 0 & 0 \\ -i & 0 & 0 \end{bmatrix}, \quad \hat{S}_t = \begin{bmatrix} 0 & -i & 0 \\ i & 0 & 0 \\ 0 & 0 & 0 \end{bmatrix}. \quad (10)$$

Here, the wave vector $|\psi_{\mathbf{v}}(s)\rangle$ is not necessarily normalized. Its length does not change since the matrix $\hat{H}(s)$ is Hermitian. The instantaneous eigen states of $\hat{H}(s)$ are given by

$$|0\rangle = [0, -\sin \theta(s), \cos \theta(s)]^T, \quad (11)$$

$$|+1\rangle = \frac{1}{\sqrt{2}} [-i, \cos \theta(s), \sin \theta(s)]^T, \quad (12)$$

$$|-1\rangle = \frac{1}{\sqrt{2}} [i, \cos \theta(s), \sin \theta(s)]^T, \quad (13)$$

with corresponding eigenvalues 0 and $\pm\omega(s)$. We note that the curvature $\kappa(s)$, torsion $\tau(s)$, $\omega(s) = \sqrt{\kappa^2(s) + \tau^2(s)}$, and the pitch angle $\theta(s)$ are all dependent on s for a non-uniform helix.

Now, we verify that the vector \mathbf{v} always returns to its initial value after an adiabatic circulation. Round a close curve C in the \mathbf{B} -parameter space [see Fig. 1 (b)], the eigen state $|n\rangle$ ($n = 0, \pm 1$) of \hat{H} will accumulate both the dynamical phase $\alpha_n(C)$ and the Berry's phase $\gamma_n(C)$ [3]. The Berry's phases for all three states are zero because the corresponding solid angle $\Omega_n(C)$ in the parameter space vanishes as shown in Fig. 1 (b). The dynamics phase for the three states are given by

$$\alpha_n(C) = -n \int_C \omega(s) ds = -n \int_0^{2\pi} d\varphi = -2n\pi, \quad n = 0, \pm 1, \quad (14)$$

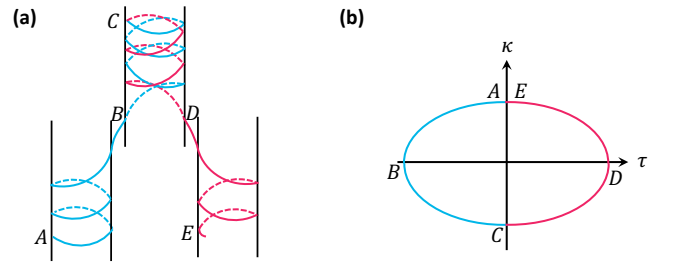


FIG. 2. (a) A winding method of a fiber to obtain non-vanishing Berry's phase for the local coordinate frame (LCF). (b) The path of the LCF in the parameter space. At points B and D , the curvature $\kappa(s)$ of the curve changes sign. At point C , the sign of the torsion $\tau(s)$ of the curve flips.

where we have used the geometric relation $\omega(s)ds = d\varphi$ for each small segment. By expanding $|\psi_{\mathbf{v}}\rangle$ with $|n\rangle$, we can verify that $|\psi_{\mathbf{v}}(\varphi = 2\pi)\rangle = |\psi_{\mathbf{v}}(\varphi = 0)\rangle$. Thus, in the laboratory reference frame, \mathbf{v} returns to its initial value round C , i.e., $\mathbf{v}(\varphi = 2\pi) = \mathbf{v}(\varphi = 0)$. This proves our claim that the LCF remains the same after an adiabatic circulation.

In principle, we can construct a complicated winding path, such that the Berry's for the LCF is not zero as shown in Fig. 2. Special care needs to be taken at points B and D , at which the curvature $\kappa(s)$ vanishes and the normal vector \mathbf{n} is not defined. More details about the non-vanishing Berry's phase are out of our interest in this work. Next, we focus on the rotation of the PCF with respect to the LCF.

Rotation of the photon coordinate frame—The wave vector \mathbf{k} and two transverse polarization unit vectors (\mathbf{e}_1 and \mathbf{e}_2) form another coordinate frame—the PCF [see Fig. 3 (a)], which co-moves with the photon. We emphasize that the PCF is not synchronized with the LCF usually. This de-synchronization leads to the rotation of the linear polarization vector of the photon and the geometric phase for circularly polarized light. We note that it is invalid to evaluate the propagating phase factor via ray optics $\exp(i\mathbf{k} \cdot \mathbf{r})$ for single-mode fibers. However, the propagating phase is irrelevant to our concerned problem [4]. Here, we assume that the adiabatic change of the wave vector \mathbf{k} in a fiber can be treated as successive reflections in fibers. Previous experimental results [1, 5] can be perfectly explained with our pure geometric approach. The validity of our assumption will further be verified by measuring our predicted geometric phase for twisted photons as shown in the next section.

Two successive reflections of the photon give an adiabatic transformation of the PCF in the fiber as shown in Fig. 3 (a). Now we sit on the LCF to study the dynamics of an arbitrary vector \mathbf{v} co-moving with the PCF. The reflection of the PCF at s is described by the matrix

$$\hat{P}_t = \begin{bmatrix} -1 & 0 & 0 \\ 0 & -1 & 0 \\ 0 & 0 & 1 \end{bmatrix}, \quad (15)$$

which is the space reversion in the normal plane (i.e., \mathbf{nb} -plane). Here, we have used the fact that the no rotation of the PCF around the \mathbf{k} -axis occurs under a reflection as shown

in Fig. 3 (b). From s to $s + ds/2$, the vector \mathbf{v} itself remains unchanged. However, the LCF has been rotated by $\hat{R}(\Delta\varphi/2, \mathbf{e}(s))$. Thus, from the perspective of the LCF, \mathbf{v} has been rotated by $\hat{R}(-\Delta\varphi/2, \mathbf{e}(s))$. Here, we see an infinitesimal adiabatic evolution of the PCF is described by

$$\hat{U}(\Delta\varphi) = \hat{R}\left(-\frac{\Delta\varphi}{2}, \mathbf{e}(s)\right) \hat{P}_t \hat{R}\left(-\frac{\Delta\varphi}{2}, \mathbf{e}(s)\right) \hat{P}_t. \quad (16)$$

If a fiber is wound in a co-planar path (i.e., $\tau(s) = 0$), the photon polarization vector propagates by parallel transport as the same as the LCF. This was taken as an axiom by Ross and supported by his experiment [1]. Haldane pointed out this claim follows geometrically by approximating a general fiber path as a sequence of curved co-planar segments joined by straight segments [10]. We now verify this result directly by setting $\theta = \pi/2$ in Eq. (16). We find that the adiabatic evolution operator always equals the identity matrix, i.e., $\hat{U}(\Delta\varphi) = \hat{I}$. Thus, in the absence of torsion, the PCF maintains synchronization with the LCF.

Now we show that in the presence of torsion, the vector \mathbf{v} co-moving with the PCF rotates around the \mathbf{t} -axis during propagation. The motion equation of $\mathbf{v}(\varphi)$ in the LCF is given by

$$\frac{d}{d\varphi} \mathbf{v}(\varphi) = \hat{\mathcal{H}}(\varphi) \mathbf{v}, \quad (17)$$

where

$$\hat{\mathcal{H}}(\varphi) = \lim_{\Delta\varphi \rightarrow 0} \frac{\hat{U}(\Delta\varphi) - \hat{I}}{\Delta\varphi} = \begin{bmatrix} 0 & \cos \theta(\varphi) & 0 \\ -\cos \theta(\varphi) & 0 & 0 \\ 0 & 0 & 0 \end{bmatrix}. \quad (18)$$

The dynamics of the vector $\mathbf{v}(\varphi)$ co-moving with the photon is given by the evolution operator

$$\hat{U}(\varphi) = \begin{bmatrix} \cos \alpha(\varphi) & \sin \alpha(\varphi) & 0 \\ -\sin \alpha(\varphi) & \cos \alpha(\varphi) & 0 \\ 0 & 0 & 1 \end{bmatrix}, \quad (19)$$

with $\alpha(\varphi) = \int_0^\varphi \cos \theta(\varphi') d\varphi'$. We see that $\hat{U}(\varphi)$ describes the rotation around \mathbf{t} -axis by angle $\alpha(\varphi)$. The evolution operator can be obtained by re-expressed Eq. (17) as an effective Schrödinger equation. Then, the corresponding evolution operator is given by $\hat{U}(\varphi) = \hat{M} \hat{\Lambda}(\varphi) \hat{M}^\dagger$ with

$$\hat{M} = \frac{1}{\sqrt{2}} \begin{bmatrix} 1 & 1 & 0 \\ i & -i & 0 \\ 0 & 0 & \sqrt{2} \end{bmatrix}, \quad (20)$$

formed by the eigen vectors of $i\hat{\mathcal{H}}(\varphi)$ and the diagonal matrix carrying the dynamic phase

$$\hat{\Lambda}(\varphi) = \begin{bmatrix} e^{i\alpha(\varphi)} & 0 & 0 \\ 0 & e^{-i\alpha(\varphi)} & 0 \\ 0 & 0 & 1 \end{bmatrix}. \quad (21)$$

For a single-mode fiber, we assume that the photon enters the fiber nearly parallel to its tangent vector, i.e., $\mathbf{k}(0)/|\mathbf{k}| \approx$

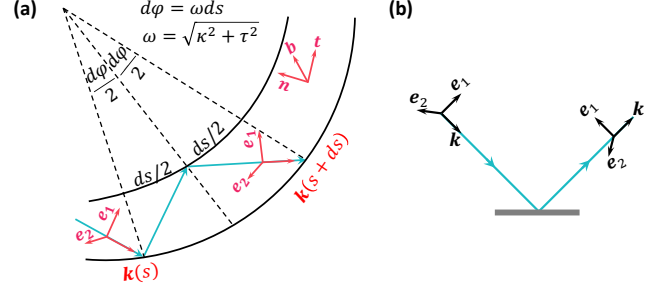


FIG. 3. (a) Two successive reflections in the fiber give an adiabatic transformation of the photon coordinate frame (PCF). (b) The change of the PCF under a reflection.

$\mathbf{t}(0)$. The PCF and LCF coincide at the beginning. It follows that the rotation angle of the polarization vector, i.e., the geometric phase for the circularly polarized light after an adiabatic circulation is given by

$$\gamma_{\pm}(C) = \pm\alpha(2\pi) = \pm \int_0^{2\pi} \cos \theta(\varphi) d\varphi. \quad (22)$$

This explains Tomita and Chiao's experiment [5]. For a uniform helix, the pitch angle θ is a constant. Then our phase geometric phase $\gamma_{\pm}(C) = \pm 2\pi \cos \theta$ recovers Chiao and Wu's results [4]. We emphasize that, in our description, $\gamma_{\pm}(C)$ is due to the purely classical rotation between the two coordinate frames and it is not the quantum Berry's phase. Even if we treat Eq. (17) as an effective Schrödinger equation, this phase corresponds to the dynamic phase not Berry's phase.

Geometric phase for a twisted photon—The upper analysis is not limited to single-mode fibers. We now apply our method to a twisted photon carrying non-zero OAM traveling in a coiled few-mode or multi-mode fiber. We show that the geometric rotation also occurs on the OAM states. The corresponding geometric phase for a twisted photon carry $m\hbar$ OAM is given by

$$\gamma_m(C) = m \int_0^{2\pi} \cos \theta(\varphi) d\varphi, \quad (23)$$

which is m times as large as that of a photon spin state.

A linearly polarized twisted optical pulse or beam propagating in the z -direction can be generally described by a spectral amplitude function in \mathbf{k} -space [8, 12]

$$\xi_m(\mathbf{k}) = \eta(k_z, \rho_k) e^{im\phi_k}, \quad (24)$$

where $\rho_k = \sqrt{k_x^2 + k_y^2}$, ϕ_k is the azimuthal angle of \mathbf{k} in the PCF, m is an integer determining the OAM quantum number, and the function η characterizes the spacial distribution of the photon. As shown in the previous section, any vector co-moving with the PCF will be rotated around the \mathbf{t} -axis via $\hat{U}(\varphi)$. Usually, the beam is injected into the fiber along \mathbf{t} -axis, i.e., $\mathbf{e}_z \approx \mathbf{t}(0)$. We now let the LCF and the PCF coincide with each other at the beginning $\varphi = 0$, i.e., $\mathbf{e}_x = \mathbf{n}(0)$ and $\mathbf{e}_y = \mathbf{b}(0)$. Applying the evolution operator $\hat{U}(\varphi)$ on the vector

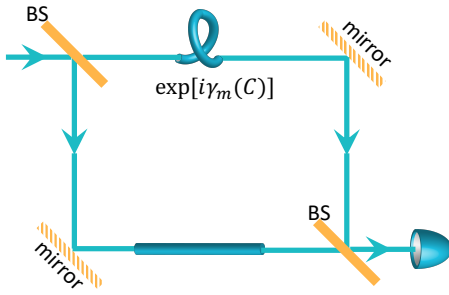


FIG. 4. Detection of the geometric phase $\gamma_m(C)$ for twisting photons carrying orbital angular momentum via Mach-Zehnder interference. In experiments, an extra Dove prism will be added in the lower optical path after the first beam splitter (BS).

\mathbf{k} , we have the components of \mathbf{k} in the LCF,

$$k_n(\varphi) = k_x \cos \alpha(\varphi) + k_y \sin \alpha(\varphi), \quad (25)$$

$$k_b(\varphi) = -k_x \sin \alpha(\varphi) + k_y \cos \alpha(\varphi), \quad (26)$$

$$k_t(\varphi) = k_z. \quad (27)$$

and the transformation relation

$$(k_x + ik_y)^m \rightarrow [k_n(\varphi) + ik_b(\varphi)]^m \exp[i m \alpha(\varphi)]. \quad (28)$$

The LCP returns to its initial configuration after an adiabatic circulation, i.e., $\mathbf{n}(2\pi) = \mathbf{e}_x$, $\mathbf{b}(2\pi) = \mathbf{e}_y$, $\mathbf{t}(2\pi) = \mathbf{e}_z$. Then, we have

$$(k_x + ik_y)^m \xrightarrow{\varphi=2\pi} (k_x + ik_y)^m \exp[i\gamma_m(C)]. \quad (29)$$

By re-expressing the phase factor $\exp(im\varphi_k) = [(k_x + ik_y)/\rho_k]^m$, we obtain the geometric phase in Eq. (23) for $\xi_m(\mathbf{k})$. After a Fourier transformation, this phase factor $\exp[i\gamma_m(C)]$ transfers to the corresponding wave-packet function in the real-space [13].

Now we shed light on the geometric phase for OAM modes in optical fibers. The electric field of a linearly polarized OAM mode in optical fibers can be separated into radial-dependent, propagating-phase, and azimuthal-dependent parts [14, 15],

$$\mathbf{E}(\rho, \phi, z, t) = \boldsymbol{\varepsilon}(\rho) \exp(i\beta z - \omega_0 t) e^{im\phi} \quad (30)$$

where the vector $\boldsymbol{\varepsilon}(\rho)$ characterizes the polarization and radial distribution of the electric field, ω_0 is the center frequency of

the fiber mode, and β the propagation constant [14]. After a Fourier transformation, we have

$$\mathbf{E}(\rho_k, \phi_k, k_z, t) \propto e^{im\phi_k}. \quad (31)$$

Similarly, the OAM mode function will accumulate an geometric phase $\gamma_m(C)$ after an adiabatic circulation. We note that ray optics is usually not valid to evaluate the propagating phase βz of fiber modes. However, the propagating phase is irrelevant to our concerned geometric phase $\gamma_m(C)$, which purely comes from the helical phase factor $\exp(im\phi)$ due to the classical geometric rotation between the LCF and the PCF.

Measuring geometric phase $\gamma_m(C)$ via interference experiments—Our predicted geometric phase in Eq. (23) can be observed in optical interference experiments, such as the Mach-Zehnder interference with an OAM laser beam as shown in Fig. 4. There are a straight fiber and a coiled fiber with equal length in the two interference channels, respectively. Our geometric phase $\gamma_m(C)$ will lead to the rotation of the interference petals pattern [16].

The Mach-Zehnder interference of twisted laser beams has been widely studied in experiments [17, 18]. We note that in the twisted-light Mach-Zehnder interference, an extra Dove prism is employed to reverse the sign of the OAM quantum number in one of the optical path. Thus, the photon number density measured at the output port is given by

$$\langle \hat{\psi}^\dagger(\mathbf{r}) \hat{\psi}(\mathbf{r}) \rangle \propto |\exp[im\varphi + i\gamma_m(C)] + \exp(-im\varphi)|^2, \quad (32)$$

where $\hat{\psi}(\mathbf{r})$ is the effective field operator of the paraxial laser beam [13]. Here, we see that the geometric phase difference $\gamma_m(C)$ between a straight fiber and a coiled fiber leads to the rotation of the interference pattern. Similar analysis can be applied to a Mach-Zehnder interferometer with entangled twisted photons [19].

Discussion—Finally, we note that our predicted geometric phase $\gamma_m(C)$ can be utilized to construct a Z-gate for OAM-state based quantum computation [20], which has been previously realized via a pair of Dove prisms [21–23]. Previously, entangled twisted photons has been exploited for the super-sensitive measurement of angular displacements [19]. The geometric phase for twisted photons can be used to detect the pitch-angle-related quantities with higher sensitivity via a similar interference strategy.

Acknowledgments. The author thanks Professor C. P. Sun for bringing my attention to this issue. This work is funded by National Key R&D Program of China (Grant No. 2021YFE0193500).

-
- [1] J. Ross, The rotation of the polarization in low birefringence monomode optical fibres due to geometric effects, *Optical and Quantum electronics* **16**, 455 (1984).
 [2] M. Varnham, D. Payne, and R. Birch, Helical-core circularly-birefringent fibres, in *5th European Conference on Optical Communication (ECOC)* (Venice, Italy, 1985) pp. 135–138.
 [3] M. V. Berry, Quantal phase factors accompanying adiabatic

- changes, *Proceedings of the Royal Society of London. A. Mathematical and Physical Sciences* **392**, 45 (1984).
 [4] R. Y. Chiao and Y.-S. Wu, Manifestations of berry's topological phase for the photon, *Phys. Rev. Lett.* **57**, 933 (1986).
 [5] A. Tomita and R. Y. Chiao, Observation of berry's topological phase by use of an optical fiber, *Phys. Rev. Lett.* **57**, 937 (1986).
 [6] M. V. Berry, Quantum adiabatic anholonomy, in *Anomalies*

- phases, defects*, edited by U. M. Bregola, M. G., and M. G. (Bibliopolis, Naples, 1990) pp. 125–181.
- [7] L. Allen, M. W. Beijersbergen, R. J. C. Spreeuw, and J. P. Woerdman, Orbital angular momentum of light and the transformation of laguerre-gaussian laser modes, *Phys. Rev. A* **45**, 8185 (1992).
- [8] L.-P. Yang and Z. Jacob, Non-classical photonic spin texture of quantum structured light, *Communications Physics* **4**, 221 (2021).
- [9] M. Berry, Interpreting the anholonomy of coiled light, *Nature* **326**, 277 (1987).
- [10] F. Haldane, Path dependence of the geometric rotation of polarization in optical fibers, *Optics letters* **11**, 730 (1986).
- [11] M. P. Do Carmo, *Differential geometry of curves and surfaces: revised and updated second edition* (Courier Dover Publications, 2016) Chap. 1.
- [12] J. Enderlein and F. Pampaloni, Unified operator approach for deriving hermite-gaussian and laguerre-gaussian laser modes, *JOSA A* **21**, 1553 (2004).
- [13] L.-P. Yang and D. Xu, Quantum theory of photonic vortices and quantum statistics of twisted photons, *Phys. Rev. A* **105**, 023723 (2022).
- [14] A. Alexeyev, T. Fadeyeva, A. Volyar, and M. Soskin, Optical vortices and the flow of their angular momentum in a multimode fiber, *Semiconductor Physics Quantum Electronics & Optoelectronics* (1998).
- [15] C. Brunet and L. A. Rusch, Optical fibers for the transmission of orbital angular momentum modes, *Optical Fiber Technology* **35**, 2 (2017).
- [16] X. Guo, Z. Meng, J. Li, J.-Z. Yang, M. Aili, and A.-N. Zhang, The interference properties of single-photon vortex beams in mach-zehnder interferometer, *Applied Physics Letters* **119**, 011103 (2021).
- [17] J. Guo, B. Guo, R. Fan, W. Zhang, Y. Wang, L. Zhang, and P. Zhang, Measuring topological charges of Laguerre-Gaussian vortex beams using two improved Mach-Zehnder interferometers, *Optical Engineering* **55**, 1 (2016).
- [18] P. Kumar and N. K. Nishchal, Modified mach-zehnder interferometer for determining the high-order topological charge of laguerre-gaussian vortex beams, *J. Opt. Soc. Am. A* **36**, 1447 (2019).
- [19] A. K. Jha, G. S. Agarwal, and R. W. Boyd, Supersensitive measurement of angular displacements using entangled photons, *Phys. Rev. A* **83**, 053829 (2011).
- [20] A. Babazadeh, M. Erhard, F. Wang, M. Malik, R. Nouroozi, M. Krenn, and A. Zeilinger, High-dimensional single-photon quantum gates: Concepts and experiments, *Phys. Rev. Lett.* **119**, 180510 (2017).
- [21] A. De Oliveira, S. Walborn, and C. Monken, Implementing the deutsch algorithm with polarization and transverse spatial modes, *Journal of Optics B: Quantum and Semiclassical Optics* **7**, 288 (2005).
- [22] X. L. Wang, X. D. Cai, Z. E. Su, M. C. Chen, D. Wu, L. Li, N. L. Liu, C. Y. Lu, and J. W. Pan, Quantum teleportation of multiple degrees of freedom of a single photon, *Nature* **518**, 516 (2015).
- [23] Y. Zhang, F. S. Roux, T. Konrad, M. Agnew, and A. Forbes, Engineering two-photon high-dimensional states through quantum interference, *Science Advances* **2**, e1501165 (2016).